# Growing correlations and aging of an elastic line in a random potential

José Luis Iguain,[1] Sebastian Bustingorry,[2] Alejandro B. Kolton,[2] and Leticia F. Cugliandolo[3]
[1]*Departamento de Física, FCEyN, Universidad Nacional de Mar del Plata, and Instituto de Investigaciones Físicas de Mar del Plata (CONICET-UNMdP), Deán Funes 3350, 7600 Mar del Plata, Argentina*
[2]*CONICET, Centro Atómico Bariloche–Comisión Nacional de Energía Atómica, Av. Bustillo 9500, 8400 San Carlos de Bariloche, Río Negro, Argentina*
[3]*Université Pierre et Marie Curie–Paris VI, LPTHE UMR 7589, 4 Place Jussieu, 75252 Paris Cedex 05, France*
(Received 27 March 2009; revised manuscript received 23 July 2009; published 9 September 2009)

We study the thermally assisted relaxation of a directed elastic line in a two-dimensional quenched random potential by solving numerically the Edwards-Wilkinson equation and the Monte Carlo dynamics of a solid-on-solid lattice model. We show that the aging dynamics is governed by a growing correlation length displaying two regimes: an initial thermally dominated power-law growth which crosses over, at a static temperature-dependent correlation length $L_T \sim T^3$, to a logarithmic growth consistent with an algebraic growth of barriers. We present scaling arguments to deal with the crossover-induced geometrical and dynamical effects. This analysis allows us to explain why the results of most numerical studies so far have been described with effective power laws and also permits us to determine the observed anomalous temperature dependence of the characteristic growth exponents. We argue that a similar mechanism should be at work in other disordered systems. We generalize the Family-Vicsek stationary scaling law to describe the roughness by incorporating the waiting-time dependence or age of the initial configuration. The analysis of the two-time linear response and correlation functions shows that a well-defined effective temperature exists in the power-law regime. Finally, we discuss the relevance of our results for the slow dynamics of vortex glasses in high-$T_c$ superconductors.

DOI: 10.1103/PhysRevB.80.094201 PACS number(s): 74.25.Qt, 75.60.Ch, 64.70.kj, 64.60.Ht

## I. INTRODUCTION

Disordered elastic manifolds play an important role in a variety of physical systems. Growing surfaces,[1] interfaces in domain growth phenomena and phase separation,[2] and cracks in brittle materials[3] are usually viewed as elastic objects. Interesting one-dimensional realizations are polymers[4] and vortex flux lines in type-II superconductors.[5] While polymers can wrap, vortex flux lines are preferentially directed along the applied magnetic field.

A number of systems involving one-dimensional elastic manifolds display glassy features. An ensemble of interacting polymers forms a polymer melt that undergoes a glass transition.[4] The competition between vortex repulsion and their pinning to randomly located impurities also leads to glassy phases in superconductors.[5] While in the former case disorder is self-induced, in the latter the effect of the impurities is mimicked by a quenched random potential.

The relaxation dynamics of a model of layered high-$T_c$ superconductors was recently studied in Ref. 6. The magnetic vortices are considered to be directed along one direction and they can move in two transverse directions. Conventionally, this is a $(d=1)+(N=2)$-dimensional model. The dynamics following a rapid quench from the liquid state to a set of control parameters in which the equilibrium state is expected to be the so-called "vortex glass"[5] was monitored. By using numerical simulations a slow out of equilibrium relaxation typical of glasses was found. In this system, diffusive aging of the averaged two-time roughness, $\langle w^2 \rangle$, and displacement, $\langle B \rangle$, was observed. The aging was characterized by a *multiplicative* scaling form $\ell^{2\zeta}(t_w) f_{w^2,B}[\ell(t)/\ell(t_w)]$, where $\ell(t)$ is a growing characteristic length. The scaling functions $f_{w^2}$ and $f_B$ are different but the exponent $\zeta$ does not depend on the observable ($w^2$ or $B$). Besides, the system of interacting lines was perturbed in order to compute the integrated linear response, and a diffusive aging was also found, characterized by a scaling function of the type $\ell^{2\zeta}(t_w) f_\chi[\ell(t)/\ell(t_w)]$ with the *same* exponent $\zeta$ and growing length $\ell(t)$ found for the unperturbed two-time observables (roughness and displacement). It was also shown that correlation and response functions can be related by a modified fluctuation-dissipation relation after removing the "diffusive" contribution, i.e., the factors $\ell^{2\zeta}(t_w)$. This violation of the fluctuation-dissipation relation can be characterized by a *finite* effective temperature, $T_{\rm eff}$.[7,8] Furthermore, within the time window that was numerically explored, the growing length $\ell(t)$ is well described by a power law, $\ell(t) \sim t^{1/z}$. This could well be a *preasymptotic* regime after which the growing length crosses over to the expected activated dynamics logarithmic growth [when disorder free-energy barriers scale as $\Delta(L) \sim L^\psi$ with $\psi > 0$]. It is worth mentioning that although aging in high-[9] and low-$T_c$ (Ref. 10) superconductor samples has been reported in the literature, a detailed comparison to the results listed above remains to be done.

The model system used to describe vortex lines in high-temperature superconductors contains several contributions coming from different energy scales. The main contributions are the elastic energy of the individual lines, the nonlinear terms in the elastic energy, the interaction between the lines, and the quenched random pinning potential. It is clearly important to establish whether all the above listed contributions to the energy are necessary to get such aging behavior or whether similar features arise when some of the terms—nonlinear contributions to the elasticity, interactions between the lines, or random potential—are switched off. We review below the out of equilibrium dynamics of related models with and without this type of interactions.

 

The first studies of the out of equilibrium dynamics of directed elastic manifolds in a quenched random environment focused on *mean-field* models in which the transverse space is infinitely dimensional, $N\to\infty$, each transverse coordinate has infinite length, $M\to\infty$, and the manifold has finite dimension, $d$, and infinite length in all directions, $L\to\infty$.[11] This model includes only two of the energetic contributions listed above, viz., elasticity and quenched disorder, and neglects nonlinear terms and interactions between the elastic objects. A dynamic phase transition separating a liquid (high-temperature) phase from a glassy (low-temperature) one was found for all internal dimension $d$ including $d=0$.[11] Different aging dynamics characterize the low-temperature phase depending on the short or long-range character of the random potential correlations. In both cases the aging regime lasts forever (after having taken the $N\to\infty$, $M\to\infty$, and $L\to\infty$ limits): there is no multiplicative factor $\ell^{2\zeta}(t)$ in the averaged two-time observables. For short-range correlated potentials the displacement, roughness, and linear responses scale as $f_{w^2,B,\chi}[\ell(t)/\ell(t_w)]$ and a single finite effective temperature exists.

Soon after Barrat[12] and Yoshino[13,14] studied a solid-on-solid (SOS) model of a single directed elastic line relaxing with Monte Carlo (MC) dynamics on a disordered substrate with one ($N=1$) transverse direction. This system models elasticity in a rather extreme way, using a hard constrain, and includes quenched randomness. There are no interactions between different lines in this model. These authors focused on the very long length limit in an effectively infinite box ($M\gg L\gg a$ with $a$ as the lattice spacing) and found that this lattice model has a similar averaged dynamics to the one found later in the vortex glass[6] below a crossover temperature. The relaxation is slow, and the global displacement and linear response show nontrivial diffusive aging with multiplicative scaling. The characteristic length scale also appears to be a power law of time within the numerical time window and the exponents $z$ and $\alpha=\zeta/z$ are temperature and disorder strength dependent with the same qualitative trend as in the fully interacting case. More recently, we focused on the analysis of the averaged and fluctuating two-time roughness of such solid-on-solid lines with *finite length*, $L<\infty$.[15] On the one hand, we found that the aging regime stops and crosses over to saturation of the two-time roughness and free diffusion of the displacement at a characteristic value of the time delay, $\Delta t\equiv t-t_w=t_x$, which grows with the length of the line and smoothly depends on other parameters in the model. The saturation of the two-time roughness is well described by a generalization of the equilibrium Family-Vicsek scaling.[16] On the other hand, the two-time roughness fluctuations are highly nontrivial but can be characterized with a relatively simple argument by a scaling function.

The numerical solution to the Langevin equation for free lines in $N=2$ transverse dimensions[6] and, especially, the full analytic solution to the Langevin dynamics of finite Edwards-Wilkinson (EW) elastic lines[17] in one transverse dimension[18,19] ($N=1$) had also been considered, without taking into account interactions, nonlinear terms, and quenched randomness. The results suggested that not even disorder is necessary to obtain similar averaged and fluctuating aging dynamics of fully relaxing quantities. The aging scaling and saturation phenomenon of the averaged two-time roughness follow the same scaling laws as above with growing length $\ell(t)\sim t^{1/z}$ and temperature-independent exponents $z=2$, $\zeta=1/2$, and $\alpha=\zeta/z=1/4$. However, the noise-averaged linear response is stationary in this "quadratic" model. When it comes to analyzing fluctuations other differences appear. The distribution of the two-time roughness satisfies a similar scaling law as in the disordered problem although with a rather different scaling function and the linear response simply does not fluctuate.

The effect of nonlinear terms has been considered by Bustingorry[20,21] who analyzed the relaxation dynamics of "clean" finite length ($L<\infty$) Kardar-Parisi-Zhang (KPZ) lines[22] in $N=1$ transverse dimensions. In this work correlations were analyzed in detail and undergo diffusive aging with the KPZ exponents $\zeta$, $\alpha$, and $z$. The two-time and length scaling of averaged quantities and the scaling form of the probability distribution functions proposed in Ref. 15 were thus confirmed.

Finally, once the elastic lines are allowed to wrap, biologically motivated dynamic problems can also be addressed. A recent study concentrates on the effects of confinement on the out of equilibrium relaxation of a single polymer chain in two dimensions,[23] a problem of relevance for cellular modeling. Another study analyzes numerically the effect of randomly applied forces on an ensemble of interacting polymer lines, focusing on out of equilibrium properties of active matter.[24] There is, certainly, much room for further investigations in the biological context.

In this paper we return to the problem of the relaxation of directed elastic lines in the presence of quenched randomness. Interactions among different lines and nonlinear terms are not considered here. Our aim is to complete the analysis of the averaged two-time observables. In order to compare with previous results and to extract the universal behavior we treat two models in parallel: the Monte Carlo dynamics of the disordered solid-on-solid model[12–14] and the Langevin dynamics of the disordered Edwards-Wilkinson equation in $(1+1)$ dimensions. In Sec. II we define these models and we describe the numerical method and two-time observables on which we focus.

We first study in Sec. III the (correlation) growth regime of the considered models as is typically analyzed in nondisordered systems.[1] Within this context, the notion of a characteristic crossover length between thermally and disorder-dominated regimes arises naturally. Besides, we consider in detail the growth with its roughness and dynamic exponents and we confirm the existence of a crossover from power law to logarithmic growth that is, however, only observed for sufficiently large lines. Second, in Sec. IV we focus on the aging behavior of the averaged dynamics of correlation and linear response functions for different initial conditions. Special attention is paid to two-time scaling and finite-size and finite- time effects. Third, we expose in Sec. V some scaling arguments aimed to explain many of the crossover-induced effects observed in the numerical results. Finally, in Sec. VI we present our conclusions.

## II. MODELS

In this section we introduce the models and the numerical methods used to study their relaxation.

### A. Lattice model

A discrete model of a one-dimensional directed elastic object represents the line as a lattice string of length $L$ directed along the $y$ direction.[12–15] The line can move transversely along the $x$ direction on a rectangular square lattice of transverse size $M=10^4 \gg L^{2/3}$ ensuring the existence of many nearly equivalent quasiground states. The line segments, $x(y)$ $(y=1,\ldots,L)$, obey the restricted SOS rule $|x(y)-x(y-1)|=0,1$. A quenched random potential $V$ taking independent values on each lattice site is drawn from a uniform distribution in $[-1,1]$. We use $10^5-10^7$ realizations of the quenched randomness depending on the value of $L$. At each microscopic time step we attempt a move of a randomly chosen segment to one of its neighbors restricted by the SOS condition and we accept it with the heat-bath rule. One Monte Carlo step is defined as $L$ update attempts. We use angular brackets to indicate the average over thermal noise realizations. We choose two types of initial conditions: equilibrium at high temperature obtained after evolving a random initial condition during a sufficiently long-time interval at high temperature and equilibrium at zero temperature.

The lattice model has no finite elastic energy. Elasticity is modeled in an extreme way; in the absence of disorder all configurations have equal vanishing energy but the displacement between neighboring bonds is bounded to $-1,0,1$ lattice spacings.

The control parameters are temperature, $T$, and the disorder strength, $V_0=\sqrt{[V^2]_V}$. Here and in what follows we use square brackets, $[\cdots]_V$, to indicate an average over quenched randomness. The Monte Carlo rule implies that the dynamics depend only on the ratio between these parameters, $V_0/T$. In the simulations shown here we fixed $V_0=1/3$. In the following we use adimensional time, space, and energy scales.

### B. Continuous model

The SOS model is easy to simulate but it is not simply recovered as a limit of better-known continuous problems such as the KPZ equation[20,22] or the vortex line model[6] in which elasticity is modeled in a more realistic way. For this reason we also study the disordered EW line.[1]

The disordered EW equation[17] for a scalar field $x$ representing the height of a surface over a one-dimensional substrate parametrized by the coordinate $y$ (a one-dimensional directed interface) is

$$\gamma \partial_t x(y,t) = c\partial_y^2 x(y,t) + F_p[x(y,t)] + h[x(y,t)] + \xi(y,t), \tag{1}$$

where $\xi$ is a Gaussian thermal noise with $\langle \xi(y,t)\rangle=0$ and

$$\langle \xi(y,t)\xi(y',t')\rangle = 2\gamma T\delta(y-y')\delta(t-t'). \tag{2}$$

The parameter $c$ is the elastic constant, $\gamma$ is the friction coefficient, $T$ is the temperature of the thermal bath (in energy units), and $\langle\cdots\rangle$ is the average over the white noise $\xi$, i.e., the thermal average. The Boltzmann constant has been set to 1, $k_B=1$. The term $h$ represents the effect of a perturbing field that couples linearly and locally to the height, $-h(y,t)x(y,t)$. One can also consider other types of perturbation that couple to more complicated functions of the height as defined in Sec. II D. The random pinning force $F_p[x(y,t)]=-\partial_x V(x,y)$ represents the effect of a random-bond disorder described by the potential $V(x,y)$, whose sample-to-sample fluctuations are given by

$$[(V(x,y)-V(x',y'))^2]_V = \delta(y-y')R(x-x'), \tag{3}$$

where $R(u)$ stands for a short-ranged correlator along the $x$ coordinate with range $r_f$. The continuous random potential is modeled by a cubic spline passing through $M$ regularly spaced uncorrelated Gaussian number points.[25] We adimensionalize Eq. (1) by using $r_f$ as the unit of distance in the $x$ direction, $\gamma r_f$ as the unit of time, and $V_0$ as unit of energy/temperature. The unit of distance in the longitudinal direction $y$ can be conveniently taken as the layer spacing $s$ of the numerically discretized Laplacian (such a choice is natural when modeling a layered material such as a high-$T_c$ superconductor with an external magnetic field applied perpendicular to the oxide planes). In these units, the friction and elastic coefficients are equal to 1, leaving only two independent parameters in the model: the adimensionalized elastic constant $\nu=cr_f/s^2$ and the adimensionalized temperature $T/V_0$ (from now on, we use $T$ for $T/V_0$). Finally, by choosing $\nu=1$ we focus exclusively in the temperature dependence for a fixed disorder.

We use a finite-difference algorithm to integrate the partial differential equation in which the first and second order partial derivatives are discretized in the usual way (see Ref. 20 for more details on the numerical technique). We typically simulate lines with lengths $L=64,256,1024$. The time step is $t_0=0.01$. We use $10^3$ noise realizations to evaluate the two-time averaged correlations and responses.

Note that in the continuous model each nonstrictly flat configuration has a finite elastic energy, while in the lattice model all configurations have the same vanishing elastic energy.

### C. Quenched randomness

The kind of quenched disorder used in both models is of the "random-bond" type in the sense that, for a domain wall described by our elastic interface model, it does not break the symmetry properties of the corresponding order parameter.[26] This implies that the two-dimensional disorder potential locally couples to the interface position and that $R(u)$ in Eq. (3) saturates to a constant for large distances. The way we generate the disorder corresponds to a short-ranged function $R(u)$. The effect of long-range correlated randomness has been studied in mean-field elastic manifold models[11] but we do not contemplate it here.

### D. Observables

We study the relaxation after two types of rapid changes in the control parameters. The first protocol, and the more usual one, describes a quench from high to low temperatures. After equilibration at high $T$ the system is quenched to a low value of $T$. The second protocol, less usual, consists in first equilibrating the sample at zero temperature (i.e., starting in

its ground state), $T_0=0$, and then heating the sample to a higher temperature. In both cases, the line is allowed to relax from the quench occurring at time $t=0$ until a waiting time $t_w$ when the quantities of interest are recorded and later compared to their values at subsequent times $t>t_w$.

The aging dynamics of elastic lines has been initially studied in terms of the averaged two-time mean-squared displacement $\langle B\rangle(t,t_w)=\langle[(x(y,t)-x(y,t_w))^2]_V\rangle$.[12,13] The behavior of this quantity is somehow obscured by the motion of the center of mass. We thus prefer to focus on the roughness of the lines, a quantity that has been widely used in the study of interface dynamics[1] but generalized here to include the $t$ and $t_w$ dependences. The two-time roughness is given by

$$\langle w^2\rangle(t,t_w)=\frac{1}{L}\sum_y\langle[(\delta x(y,t)-\delta x(y,t_w))^2]_V\rangle, \tag{4}$$

where $\delta x(y,t)=x(y,t)-\bar{x}(t)$ accounts for the displacement of the $y$th line segment relative to the center of mass, $\bar{x}(t)=L^{-1}\Sigma_y x(y,t)$.

The two-time structure factor is defined as[1,18]

$$\langle S_n\rangle(t,t_w)=L\langle[|c_n(t)-c_n(t_w)|^2]_V\rangle,$$

$$Lc_n(t)=\sum_y[x(y,t)-\bar{x}(t)]e^{-iq_ny}, \tag{5}$$

where $q_n=2\pi n/L$ with $n$ being an integer number.

Further insight into the dynamics of out of equilibrium systems is given by the linear response function. The latter is defined by applying a random time-independent force at a time $t_w$ on a replica of the system and by computing how this one departs from an unperturbed one evolving with the same thermal noise. Concretely, the energy contribution of a field conjugated to the displacement with respect to its mean value is

$$\mathcal{H}'^{w^2}=-h\sum_y[x(y,t)-\bar{x}(t)]s(y)\theta(\Delta t). \tag{6}$$

$s(y)=\pm 1$ with equal probability, $\langle\langle s(y)\rangle\rangle=0$, and $\langle\langle s(y)s(y')\rangle\rangle=\delta_{y,y'}$ (Ref. 27) with $\langle\langle\cdots\rangle\rangle$ denoting the average over the perturbing field distribution. $h$ is the intensity of the perturbation. The associated linear response function is

$$\langle\chi\rangle(t,t_w)=\frac{1}{hL}\sum_y\langle[(\delta x^h(y,t)-\delta x(y,t))s(y)]_V\rangle. \tag{7}$$

Henceforth $\langle\cdots\rangle$ indicates the average over the thermal noise *and* the $s(y)$ distribution.

In equilibrium the averaged linear response is related to the averaged spontaneous fluctuations of the corresponding observable by the model-independent fluctuation-dissipation theorem (FDT) which states

$$\langle w^2\rangle(\Delta t)=2T\langle\chi\rangle(\Delta t) \tag{8}$$

(the Boltzmann constant has been set to 1, $k_B=1$), where the $\Delta t$ argument implies stationary dynamics. In a system relaxing out of equilibrium this relation does not necessarily hold. In a number of glassy systems one can define an effective temperature[7] from the modification of the above relation. In the aging regime of elastic lines in disorder media the FDT is violated and one constructs the modified FDT,[6,8,13]

$$\langle w^2\rangle(t,t_w)=2T_{\rm eff}(t,t_w)\langle\chi\rangle(t,t_w), \tag{9}$$

where $T_{\rm eff}$ measures to what extent FDT is violated and has been also shown to behave in many situations as a bona-fide (nonequilibrium) time-scale dependent temperature in a thermodynamic sense.[8] The two-time dependence of the effective temperature is here kept general. It turns out that in models with multiplicative scaling, as the one discussed here, once the factors $\ell^{\zeta}(t)$ have been taken into account, the redefined effective temperature approaches a constant value (see Sec. IV C and Refs. 6, 12–14, 18, and 27).

### E. Dynamic crossover

In $(1+1)$ dimensions there is no phase transition to a high-temperature "free phase." Disorder is always relevant for an elastic string and fluctuations are always dictated by the disorder at the largest length scales. The characteristic nonequilibrium nonstationary glassy phenomenon then appears as a size-dependent dynamic crossover.[12–15,18–20] For all observation times, $t_{obs}$, which are longer than a size, disorder strength, and temperature-dependent *equilibration time*, $t_{eq}$, the system reaches equilibrium. Instead, for $t_{obs}<t_{eq}$ the relaxation is nonstationary and thus occurs out of equilibrium as demonstrated by two-time correlations and linear responses that age and violate fluctuation-dissipation theorems. The equilibration time $t_{eq}$ increases by increasing the size $L$ of the line, by decreasing the temperature $T$, and by increasing the quenched disorder strength $V_0$.

In finite systems however (which can be realized experimentally as discussed in Sec. VI), strong enough thermal fluctuations can induce a finite-size crossover at a size-dependent crossover temperature $T_{co}(L)$. At high temperature, such that $T>T_{co}(L)$, disorder is effectively washed out, the equilibration time is relatively short, and the line behaves as the clean EW one at high temperature. At equilibrium the FDT holds, and the exponents (defined and discussed below) are the ones of the clean EW line, $\alpha=1/4$, $\zeta=1/2$, and $z=2$. At lower temperatures, $T<T_{co}(L)$, the equilibration time is usually longer than the observation time and the dynamics remains nonstationary.[12–15] Thermal fluctuations induce in this case a geometrical crossover at a temperature-dependent length scale $L_T$, separating a short length-scale roughness regime described by the "thermal" exponent $\zeta_T$ from a large length-scale roughness described by a "disorder" exponent $\zeta_D$. Determining this geometrical crossover as a function of temperature is therefore important for determining the dynamic crossover in a finite system since $T_{co}(L_T)\approx T$.

## III. GROWTH AND SATURATION

In this section we recall the main tools and concepts used to analyze the evolution of the conformational properties of elastic manifolds and we generalize them to take into account the effect of the waiting time. This leads us to present the temperature dependence of the crossover length scale $L_T$.

### A. Roughness

#### 1. Comparison to the initial condition

Traditionally, the dynamics of elastic manifolds has been classified in universality classes according to the behavior of the two-time roughness [Eq. (4)] evaluated at $t_w=0$, the initial time, and using a flat initial configuration, $x(y,0)=x_0$.[1,16] The waiting time being identical to zero all two-time observables depend on $\Delta t=t$ when compared to the initial condition. Initially the roughness increases as a function of $\Delta t$, and at a characteristic time $t_x(L)$ reaches saturation at an $L$-dependent value, $\langle w_\infty^2\rangle$. This behavior is encoded in the Family-Vicsek scaling[16] that, in full generality, can be expressed as

$$\langle w^2\rangle(\Delta t) \sim g(\Delta t), \tag{10}$$

$$t_x \sim f(L), \tag{11}$$

$$\langle w_\infty^2\rangle \equiv \lim_{\Delta t \gg t_x} \langle w^2\rangle(\Delta t) \sim h(L), \tag{12}$$

with $h$, $g$, $f$ as three monotonic functions. Consistency at $\Delta t=t_x$ requires $h=f\circ g$. In the usually discussed space-time scale-invariant cases in which all functions are power laws one has

$$\langle w^2\rangle(\Delta t) \sim \Delta t^{2\alpha}, \tag{13}$$

$$t_x \sim L^z, \tag{14}$$

$$\langle w_\infty^2\rangle \sim L^{2\zeta}, \tag{15}$$

where $\alpha$ is the growth exponent, $z$ is the dynamic exponent, and $\zeta$ is the roughness exponent. Consistency implies that the three exponents are related by

$$z\alpha = \zeta. \tag{16}$$

The values of the exponents are well known in a number of cases. For the EW elastic line the exponents can be analytically computed and one finds that $\alpha=(2-d)/4$, $z=2$, and $\zeta=(2-d)/2$ for $d\leq 2$. For the nonlinear KPZ elastic line the exponents are known only numerically for general $d$. In (1+1) dimensions, however, they can be computed analytically and $\alpha=1/3$, $z=3/2$, and $\zeta=1/2$.

In the presence of quenched disorder the dependence of the asymptotic roughness $\langle w_\infty^2\rangle$ with the length of the line undergoes a crossover. For lines that are shorter than a temperature and disorder strength dependent value $L_T$ the behavior is controlled by thermal fluctuations and relation (15) holds with $\zeta=\zeta_T$, the thermal roughness exponent. This exponent is the one corresponding to the EW equation, and thus $\zeta_T=(2-d)/2$ in general and $\zeta_T=1/2$ in our (1+1)-dimensional case. In this thermally dominated scale, the dynamics is expected to be "normal" in the sense that lengths and times should be thus related by power laws of types (13)–(15) with the exponents linked by Eq. (16).

For lines longer than $L_T$, the roughness is dominated by quenched disorder and one has that Eq. (15) still holds though with a different value of the roughness exponent, $\zeta=\zeta_D$. The disorder-dominated roughness exponent $\zeta_D$ is the one characterizing the geometry of the ground state configurations, and it is expected to satisfy $\zeta_D>\zeta_T$ in general.[28] In (1+1) dimensions one has $\zeta_D=2/3$.

Once quenched disorder is present, the time evolution is expected to be driven by activation over free-energy barriers. If they scale as $U(L)\sim L^\psi$, the Arrhenius law leads to a logarithmic relation between equilibrated lengths and times that implies $t(\ell)\sim e^{\Upsilon(\ell/L_\Upsilon)^\psi/T}$ with $\Upsilon$ and $L_\Upsilon$ as some characteristic energy and length scale, respectively. One might then expect

$$\langle w^2\rangle(\Delta t) \sim \ln^{\alpha_{\ln}} \Delta t, \tag{17}$$

which for consistency implies

$$\psi\alpha_{\ln} = 2\zeta_D. \tag{18}$$

All exponents cited above are temperature independent. Some glassy systems do, however, present temperature-dependent exponents asymptotically.[29–31] Whether this behavior can occur in our system is a delicate issue, which we discuss in Sec. V.

#### 2. Comparison to an aged configuration

In simple cases in which *equilibrium* is relatively rapidly reached the initial condition should be irrelevant after the equilibration time. The same relaxational behavior is then expected, independently of the waiting time $t_w$ and the initial condition. The roughness should only depend on the time difference $\Delta t=t-t_w$ and the same functional forms should characterize growth and saturation. In an *out of equilibrium* relaxation relatively soon after preparation the growth regime acquires a waiting-time dependence and relations (10)–(12) might be generalized.

For each waiting time the two-time roughness presents two regimes as a function of $\Delta t$: it first grows until crossing over at $t_x(L)$ to saturation at a $\Delta t$ independent value. For high working temperature after a short transient the memory of the initial condition disappears, and the roughness is well described by the Family-Vicsek scaling. For low working temperatures the waiting-time dependence remains. For long lines the crossover time is long enough to see aging behavior in a sufficiently long-time window, such that we can describe it with a scaling form. Before saturation the roughness does not depend strongly on the size of the line (for sufficiently long lines) and the curves can be scaled as

$$\langle w^2\rangle(t,t_w) \sim \ell^{2\zeta}(t_w)\langle \tilde{w}^2\rangle\left(\frac{\ell(t)}{\ell(t_w)}\right). \tag{19}$$

This scaling form approaches a stationary regime in which $\langle w^2\rangle(t,t_w)\sim\ell^{2\zeta}(\Delta t)$ in the limit $\Delta t \gg t_w$ if $\langle \tilde{w}^2\rangle(u)\sim u^{2\zeta}$ for $u\gg 1$. For even longer time delays such that $\ell(\Delta t)\to L$ one finds saturation at $\langle w^2\rangle(t,t_w)\to\langle w_\infty^2\rangle\sim L^{2\zeta}$, which might indeed contain a $t_w$-dependent prefactor, as in the clean EW case.[18]

The out of equilibrium regime exists without the need of quenched randomness. We showed in Ref. 18 that the roughness in the simple EW equation satisfies scaling form (19) when the system is let evolve from an out of equilibrium initial condition and the waiting-time dependence is kept ex-

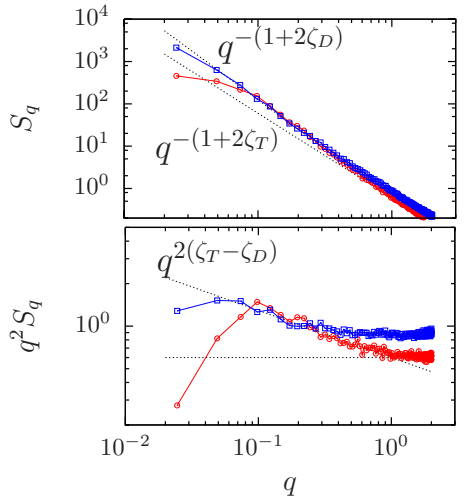


FIG. 1. (Color online) Structure factor in the continuous EW line in a random environment for $T_0=5$ and two working temperatures, $T=0.5$ (circles) and $T=0.8$ (squares), with $t_w=0$. The data show the thermal regime at very large wave vector, a crossover to a disorder-dominated regime upon decreasing the wave-vector value, and, finally, a saturation regime demonstrating that the growth length, $\ell(t)$, is shorter than the system size, $L$. In the bottom panel the structure factor is scaled by $q^2$ in order to highlight the difference between the two roughness exponents.

plicit. The length scale $\ell$ grows as $\ell(t) \sim t^{1/2}$. A similar scaling was shown numerically in Ref. 20 for the (1+1) KPZ model with $\ell(t) \sim t^{2/3}$. In Sec. IV we discuss the scaling of Eq. (19) for the disordered model.

The analysis of the saturation of the two-time roughness should, in principle, yield the thermal and disorder-dominated values of $\zeta$. Computing $\zeta$ from $\langle w^2_\infty \rangle$ is, however, numerically heavy since one needs to simulate lines with different lengths and then extract the scaling behavior. In Ref. 15 we tried such a scaling analysis but we did not reach the regime in which $\zeta=\zeta_D=2/3$ [see Fig. 1(d) in this reference]. A more convenient way of getting $\zeta$ is to study the two-time structure factor,[1] as we explain below.

### B. Structure factor

#### 1. Roughness exponents

The thermal, $\zeta_T$, and disorder, $\zeta_D$, roughness exponents can also be extracted from the analysis of the structure factor defined in Eq. (5). Working with the structure factor is convenient since it is sufficient to simulate a long chain and then extract the $L$ dependence from the wave-vector dependence.[1] Indeed, the roughness is simply related to the structure factor as

$$\langle w^2 \rangle(t,t_w) = L^{-1} \sum_{n=-\infty}^{\infty} \langle S_n \rangle(t,t_w), \tag{20}$$

and this implies that the dynamic scaling [Eqs. (10)–(12)] (for $t_w=0$) is equivalent to

$$\langle S_n \rangle(t,t_w=0) = S^{eq}(q_n) g[q_n \ell(t)] \tag{21}$$

with $S^{eq}$ as the equilibrium wave-vector dependent structure factor and $g(u) \sim u^{d+2\zeta}$ for $u \ll 1$ and $g(u) \to$ const for $u \gg 1$, with $d$ as the internal dimension of the manifold ($d=1$ for the directed line). These limits for the function $g(u)$ ensure, respectively, the equilibrated steady geometry and the memory of the flat initial condition. In the case of power-law scaling Eq. (21) becomes

$$\langle S_n \rangle(t,t_w=0) = q_n^{-(d+2\zeta)} g[q_n t^{1/z}]. \tag{22}$$

In the out of equilibrium relaxation process we are interested, $\langle S_n \rangle$ depends on two times $t$ and $t_w$. The generalized scaling form then reads

$$\langle S_n \rangle(t,t_w) = S^{eq}(q_n) G[q_n \ell(t), q_n \ell(t_w)], \tag{23}$$

which reduces to Eq. (21) for $t_w=0$ and to a similar form for $q_n \ell(t_w) \gg 1$ for all $n$, recovering stationarity in the very long waiting-time regime. For fixed $t_w$ and $t$ we can study the dependence of $\langle S_n \rangle$ on $q_n$. If the aim is to determine the values of the roughness exponent the ideal choice would be to use a very long $\Delta t \equiv t - t_w \gg t_w$ and plot $\langle S_n \rangle$ for several $t_w$'s as a function of $q_n$. This construction is to be compared with Fig. 2(b) in Ref. 18. In presence of disorder the construction should have a broken straight-line form with two exponents, $-(1+2\zeta_{T,D})$; the thermal one, $\zeta_T$, characterizing the behavior at short length scales, $q_n > q_T$, and the disorder one, $\zeta_D$, characterizing the behavior at long length scales, $q_n < q_T$. The breaking point $q_T$ defines a characteristic length $L_T \sim 1/q_T$ which should depend on $T$ and we shall discuss and evaluate its precise temperature dependence in Sec. III B 2. In an infinite (1+1)-dimensional system disorder always dominates the fluctuations at very long length scales. However, in a finite system of length $L$ once $L_T=L$ all the system is characterized by thermal fluctuations and the value of $L_T$ is thus crucial.

Studying the wave-vector dependence of the structure factor is thus a convenient way to determine the roughness exponents, $\zeta_{T,D}$; we hence expect to improve the values shown in Fig. 1(d) in Ref. 15. We studied the $t_w=0$ structure factor in the continuous disordered EW line. The general behavior described in the previous paragraphs is shown in Fig. 1 for working temperatures $T=0.5$ and $T=0.8$. Note that the saturation of the structure factor at very small wave vector bears the same information as the fact that the roughness $\langle w^2 \rangle$ has not yet saturated at the longest time shown in Fig. 1. It means that the growing correlation length has not reached the size of the system, $\ell(t) < L$. The crossover from the thermal, $\zeta_T$, to the disorder, $\zeta_D$, roughness exponents is clear, with the expected values $\zeta_T=1/2$ and $\zeta_D=2/3$ confirmed. Note that the top panel in Fig. 1 shows the raw data, while the bottom panel shows the structure factor multiplied by $q^2$, which allows us to better observe the crossover region and the difference between the two exponents.

#### 2. Crossover length scale $L_T$

The analysis of the structure factor also allows us to evaluate the temperature and disorder strength dependence of the crossover length $L_T$ (or wave vector $q_T$) and compare it to

previous numerical[14] and analytical[5,26,32] studies.

The temperature-dependent crossover length $L_T$ separating the saturation regime characterized by the thermal and disorder exponents $\zeta_T$ and $\zeta_D$ should be observable as a temperature-dependent crossover wave vector $q_T$ in the structure factor. In order to access it one then needs to use a sufficiently long-time delay in such a way that the second factor saturates to $g(u)\to$const. In this way, we dynamically determine the crossover length $L_T$, which can be related to information about the static structure of the system, as exposed below in Sec. V.

The crossover length and the crossover wave vector are expected to scale with temperature as $L_T \sim T^{1/\phi}$ and $q_T \sim T^{-1/\phi}$, with $\phi$ defining an exponent that we shall obtain below using a variety of arguments. The characteristic length scale $L_T \sim 1/q_T$ should increase with increasing temperature ($\phi > 0$), indicating that thermal fluctuations become more and more important.

A simple new "matching" argument to obtain the $\phi$ exponent relies on the fact that the average fluctuations at large enough length scales ($q_n < q_T$) are not expected to depend on the working temperature, in contrast with the short length-scale ones, and that the quasiequilibrated geometry has the same roughness exponents than in equilibrium. This is indeed confirmed in our numerical simulations, as can be observed comparing the two sets of data in Fig. 1. We will use this observation as a main input for the scaling arguments in Sec. V. Let us assume that a weak temperature dependence is permitted, i.e., $\langle S_q \rangle \sim a(T) q_n^{-(1+2\zeta_D)}$ for $q_n < q_T$, while $\langle S_q \rangle \sim T q_n^{-(1+2\zeta_T)}$ for $q_n > q_T$. Matching the crossover between these two regimes at $q_T$ one obtains

$$q_T \sim \left[ \frac{T}{a(T)} \right]^{-1/[2(\zeta_D - \zeta_T)]}. \tag{24}$$

Using $a(T) \sim a$ yields $q_T \sim T^{-1/[2(\zeta_D - \zeta_T)]}$ and $\phi = 2(\zeta_D - \zeta_T)$. With simulations of the discrete model Yoshino found $\phi = 1/3$,[14] in agreement with this result since for our one-dimensional case $\phi = 2(\zeta_D - \zeta_T) = 2(2/3 - 1/2) = 1/3$.

This simple scaling argument gives the exponent $\phi$ in terms of static roughness exponents. It should be noted that it is a consequence of two main facts: (i) the average structure factor becomes independent of $T$ for small $q$, i.e., our numerical results support $a(T) \sim a$, and (ii) the averaged quasiequilibrated structure factor is identical to the one at equilibrium. This states the relation between statics and dynamics though we are strictly studying a nonequilibrium problem.

A different prediction for the exponent $\phi$ comes from an order-of-magnitude argument. If one assumes that the characteristic *free-energy barrier*, $\Delta(L)$, associated to the length scale $L_T$ should be the thermal one,

$$\Upsilon \left( \frac{L_T}{L_0} \right)^{\psi} \sim k_B T, \tag{25}$$

one finds

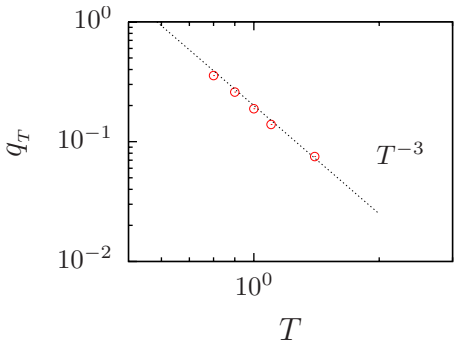


FIG. 2. (Color online) The value of the wave vector $q_T$ signaling the crossover between the thermal and disorder regimes at different working temperatures. The temperature dependence is consistent with the expected $q_T \sim T^{-3}$ power law [see Eq. (24)].

$$L_T \sim L_0 \left( \frac{k_B T}{\Upsilon} \right)^{1/\psi}. \tag{26}$$

If $\Upsilon$ and $L_0$ are independent of temperature, $L_T \sim T^{1/\psi}$ and $\phi = \psi$. Yoshino used this kind of argument with the free-energy barrier replaced by the sample-to-sample fluctuations of the free energy, an assumption that was tested in Ref. 28 for low temperatures. By replacing $\psi$ with the energy exponent $\theta$ one gets $\phi = \psi \approx \theta$ ($\theta = 1/3$ in $d = 1$).[14] This argument assumes that the scale $L_T$ is the onset for thermally activated motion, making a connection between the dynamics and the averaged static geometry of the line.

Nattermann *et al.*[26] predicted $\phi \simeq 2(\zeta_F - \zeta_T) = 1/5$ by using $\zeta_T = [3 - (d+N)]/2 = 1/2$, the thermal exponent, and $\zeta_F = [5 - (d+N)]/5 = 3/5$, the Flory roughness exponent, in $d = N = 1$. To get this result these authors defined $L_T$ as $H_{\rm dis}(L_T) \sim H_{\rm el} \sim k_B T$ by treating the disorder energy $H_{\rm dis}$ as a perturbation of the elastic Hamiltonian $H_{\rm el}$ for short length scales compared to $L_T$. Since interface fluctuations at length scales smaller than $L_T$ are expected to be Gaussian and nonrenormalized, they assumed that Flory argument should give the correct scaling behavior for $H_{\rm dis}$ at these scales. Therefore, Flory exponents should appear in the definition of $L_T$ rather than the exact roughness exponent $\zeta = 2/3$. Remarkably the same result $\phi = 1/5$ was obtained subsequently by several authors[5,32] by a simple estimation of the thermally smoothed pinning energy. Moreover, the more rigorous Gaussian variational method applied to this problem was recently found to yield the same exponent that is obtained with the simple Flory argument.[33]

The crossover between the thermal and the disorder regimes we find in the $t_w = 0$ structure factor depends, as predicted, strongly on temperature. For $T = 0.5$ and $T = 1$, for instance (using $L_T \equiv 2\pi/q_T$), we get $L_T(T = 0.5) \approx 6$ and $L_T(T = 1) \approx 45$, respectively. In Fig. 2 we show the temperature dependence of $L_T$ extracted from the $t_w = 0$ structure factor at different working temperatures. Our numerical results of the disordered EW line are thus compatible with $\phi = 1/3$ in agreement with the first two exposed arguments and Ref. 14 [see Eq. (24)], but it rules out the value 1/5 given in Refs. 5, 26, and 32. Interestingly, our results are consistent with the general prediction by Nattermann *et al.*, $\phi \simeq 2(\zeta_F - \zeta_T)$, only

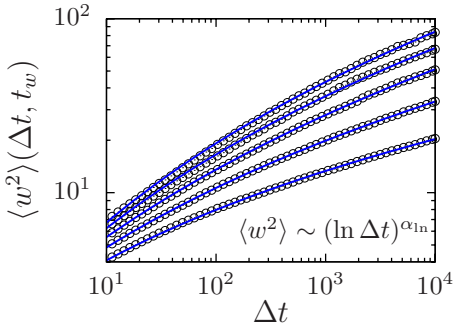


FIG. 3. (Color online) Logarithmic fit of the roughness relaxation of the elastic string with $t_w=0$. All the curves correspond to the same initial temperature $T_0=5$ and different quench temperatures $T=0.5$, 0.7, 0.9, 1.1, and 1.3 from lower to upper curves. Circles are raw data and blue continuous curves are the fitted functions.

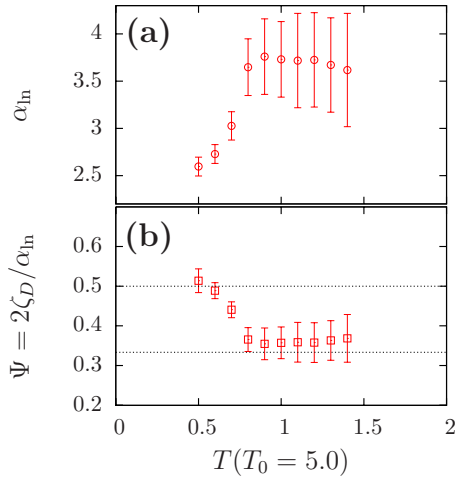


FIG. 4. (Color online) Dependence on the working temperature of (a) the $\alpha_{\ln}$ exponent obtained from the fits in Fig. 3 and (b) the barrier exponent $\psi=2\zeta_D/\alpha_{\ln}$ [see Eq. (18)], with the dotted lines indicating the suggested values $\psi=1/2$ and $\psi\approx\theta=1/3$. The temperature of the initial condition is $T_0=5.0$. The error bars were estimated from the dispersion of the exponents when changing the fitting range.

if we replace $\zeta_F=3/5$ by $\zeta=2/3$. This yields indeed the same relation that follows Eq. (24) which implies, at the same time, $\phi\simeq\theta$, where the $\theta$ is the energy static exponent. Our results thus clearly prompt for a re-examination of the different arguments given so far. In this respect in Sec. V we provide minimal matching arguments based on numerical evidence which explain several of our results and can be thus used as a benchmark for a more refined theory.

### *3. Growing length: Logarithmic growth from $t_w=0$ measurements*

At high temperature, $T>T_{co}(L)$, equilibrium is quickly reached, disorder is irrelevant, and one recovers stationary dynamics with the clean EW temperature-independent values $\alpha=1/4$, $\zeta=\zeta_T=1/2$, and $z=2$. At low temperature one has to distinguish between the thermal and disorder regimes and analyze the width of the crossover region.

We shall first take $t_w=0$ and compare with the results obtained by Kolton *et al.*[34] (see also Ref. 35). These authors showed, by studying the evolution of the structure factor of an elastic line in random media from a flat initial condition and using $t_w=0$, that the characteristic growing length crosses over from a power-law dependence $\ell(t)\sim t^{1/2}$ typical of the clean EW case to a logarithmic law, $\ell(t)\sim(\ln t)^{1/\psi}$ with $\psi\sim 0.49$ (see Fig. 2 in Ref. 34). The exponent $\psi$ characterizes the scaling of the barriers at large scales, $\Delta(L)\sim L^{\psi}$. Kolton *et al.* expected $\psi=\theta$, with $\theta$ as the exponent characterizing the free-energy cost of an excitation of length $L$, $\Delta F(L)\sim L^{\theta}$. The value of $\theta$ is known exactly for $d=N=1$, $\theta=1/3$, and Kolton *et al.*[34] ascribed the discrepancy between the measured growing length, $\ell(t)\sim(\ln t)^{1/0.49}$, and their expectation, $\ell(t)\sim\ln^3 t$, to strong logarithmic corrections.

If the structure factor scales as in Eq. (21), the roughness scales as

$$\langle w^2\rangle(\Delta t)\sim\int dq q^{-(1+2\zeta)} g[q\ell(\Delta t)]\sim\ell^{2\zeta}(\Delta t). \quad (27)$$

Using a long line, $L=256$, as in Ref. 34 we confirm the logarithmic growth of the roughness for the $t_w=0$ case, as shown in Fig. 3. Different curves correspond to increasing temperatures, $T=0.5$, 0.7, 0.9, 1.1, and 1.3, from bottom to top. We fit these curves to $\langle w^2\rangle(\Delta t)=A[\ln(\Delta t/B)]^{\alpha_{\ln}}$ obtaining the temperature-dependent $\alpha_{\ln}(T)$ exponent shown in Fig. 4(a). Now, by simply using the relation $\langle w^2\rangle(\Delta t)\sim\ell^{2\zeta}(\Delta t)\sim(\ln\Delta t)^{\alpha_{\ln}}$, one recovers the exponent $\psi$, i.e., $\psi=2\zeta_D/\alpha_{\ln}(T)$, where we assumed that in this regime the disorder roughness exponent is the relevant one. We obtain $\psi(T=0.5)\approx 0.51$ which is close to the value $\psi\approx 0.49$ obtained in Ref. 34.

Recently, Monthus and Garel[36] conjectured $\psi=d_s/2$ with $d_s$ as the dimension of the surface of the excitation, $d_s=1$ in our case, which is in very good agreement with our numerical results at $T=0.5$ without any need to advocate for logarithmic corrections. However, the analysis at different working temperatures presented here reveals that the value of $\psi$ departs from 1/2 and approaches 1/3 for increasing temperature [see Fig. 4(b)]. This is in contrary to what is expected from the argument given in Ref. 36 that is based on the role of the entropic contribution. Indeed, one would have expected the value 1/2 to prevail at high temperatures, which is the opposite trend to what we find in the numerical simulations. We shall show in Sec. V that the temperature dependence of $\psi$ observed in Fig. 4(b) can be explained as a finite-size or finite-time effects induced by the crossover.

We have also analyzed the behavior of these exponents when changing the initial temperature, while keeping $t_w=0$, that is to say, using initial conditions thermalized at different $T_0$'s. We performed the same fitting procedure keeping the working temperature fixed to $T=0.5$ and varying $T_0=2.0, 2.5, 3.0, 3.5, 4.0, 4.5, 5.0$. The resulting exponents are shown in Fig. 5. Despite the rather large fluctuations we can trust that there is no systematic dependence on the initial temperature. We conclude that the exponent values do not depend on the previous history but they do on the relaxation conditions.

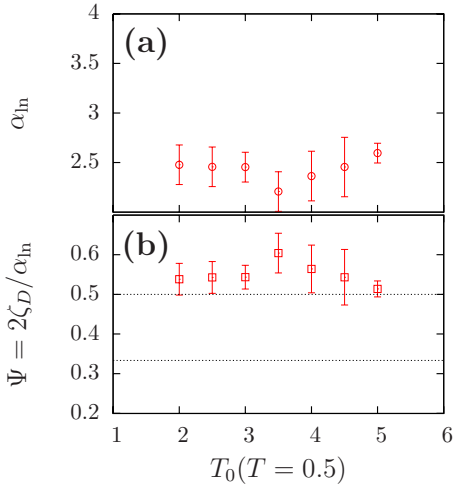


FIG. 5. (Color online) Exponents obtained from a logarithmic fit of the roughness relaxation of the elastic string for fixed working temperature $T=0.5$ and different initial conditions $T_0$. (a) $\alpha_{\rm ln}$ exponent and (b) barrier exponent, $\psi$. The dotted line indicates the suggested $\psi=1/2$ and $\psi=1/3$ values. The error bars were estimated from the dispersion of the exponents when changing the fitting range.

#### *4. Growing length: Preasymptotic power law at finite $t_w$*

When the waiting-time dependence is considered, the logarithmic growth is no longer easily observed. On the one hand, the crossover between the two asymptotic limits, $t_w \ll \Delta t$ and $t_w \gg \Delta t$, makes it difficult to fit a logarithmic growth. On the other hand, when the correlation length $\ell$ increases, the necessary time to reach the logarithmic regime increases as $t_x \sim T^6$ (see Sec. V below). Thus, from a practical point of view, in the larger system size we are able to simulate, the logarithmic regime is not reached. One can then use a power-law growth of the roughness as an effective description keeping in mind that the corresponding exponents to be used would also take effective values. We shall use such a power law to analyze the aging behavior of the roughness in Sec. IV A.

In this case, the best option to extract the dynamic growing length $\ell(t)$ is to take a very long $t_w$ and study the breaking point $q_x \sim 1/\ell$ in the structure factor. This breaking point separates the modes keeping the memory of the initial condition, $q \ll q_x$, from the equilibrated modes described by the power-law regime with disorder exponent, $q \gg q_x$. In the case of a power-law scaling, $t \sim L^z$, one has

$$q_x \sim \Delta t^{-1/z} \tag{28}$$

and from here one obtains $z$. Using power-law fits we find that the growth and dynamic exponents, $\alpha$ and $z$, acquire a $T$ dependence in the presence of quenched disorder[12–15] while the roughness exponents $\zeta_{T,D}$ do not depend on temperature.

## IV. AVERAGED AGING DYNAMICS

In this section we analyze the two-time evolution of quantities that are averaged over many realizations of the thermal noise and quenched disorder. We consider two types of preparation: cooling from a higher temperature and heating from zero temperature. We discuss how the initial condition affects the behavior in the preasymptotic growth regime.

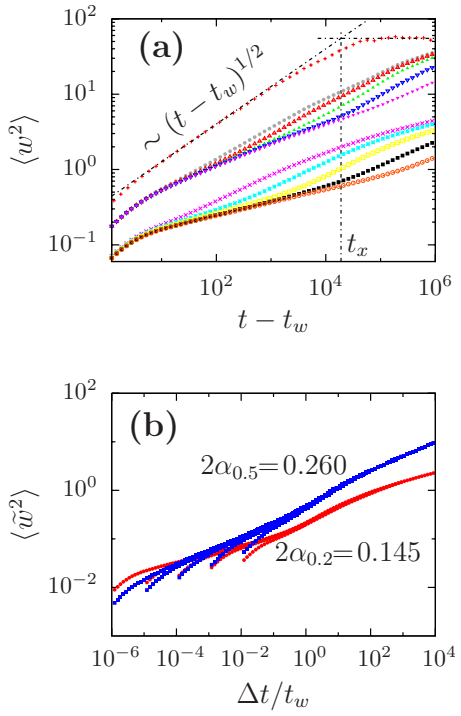


FIG. 6. (Color online) Panel (a): the noise and disorder averaged two-time roughness of the lattice elastic line with length $L=500$ evolving at $T=5, 0.5, 0.2$ after a quench from infinite temperature, $T_0 \to \infty$. Panel (b): scaling plot of the averaged two-time roughness of the line with $L=500$ and $T=0.2$ and the line with $L=5000$ and $T=0.5$.

### A. Two-time roughness

The analysis of the averaged two-time roughness of a very long line described by the solid-on-solid model following a quench from infinite temperature was given in Refs. 12–15. We summarize here these results and we complement them by showing that (i) a similar scaling form describes the relaxation dynamics of the disordered EW line, (ii) the dynamics after heating up the lines can also be described by the same scaling form with parameters that depend on the working and initial temperature, and (iii) the qualitative behavior is similar to the one found analytically for the clean EW[18,19] and numerically for the clean KPZ[20] lines.

The time-difference dependence of the averaged roughness evolving from an infinite temperature initial condition in the SOS model, for several waiting times and at three working temperatures, is shown in Fig. 6(a). The averaged roughness of the line evolving at high temperature, $T=5$, is stationary. It grows as the clean EW roughness, $\langle w^2 \rangle \sim \Delta t^{1/2}$, and it reaches saturation at $\langle w_\infty^2 \rangle$ after $\Delta t > t_x$. The line with $L=500$ evolving at $T=0.5$ is not stationary but signs of saturation are visible at $\Delta t \sim 10^6$ MCs. The line evolving at low temperature, $T=0.2$, shows aging effects, is still in the growth regime, and does not reach saturation in the numerical time window.

The averaged roughness curves in the growth regime can be well described by the scaling in Eq. (19). The numerical analysis of the growing length $\ell(t)$ in the time window we can reach indicates that $\ell(t) \sim t^{1/z}$. As discussed in Sec. III B 3 this power-law regime should be considered as a preasymptotic approximation to a slower logarithmic growth. We shall continue our analysis restricting to the power-law regime.

The resulting $t/t_w$-dependent factor $\langle \tilde{w}^2 \rangle$ [see Eq. (19)] can be well acquainted for by the empiric form[15]

$$\langle \tilde{w}^2 \rangle \left( \frac{\ell(t)}{\ell(t_w)} \right) \equiv \mathcal{G}(x) \quad \text{with} \quad x \equiv \Delta t/t_w,$$

$$\mathcal{G}(x) \sim x^{2\alpha(T)} A(T,T_0) 10^{B(T,T_0) g(x,T,T_0)},$$

$$g(x,T,T_0) \equiv \tanh\left[ C(T,T_0) \log_{10}\left( \frac{x}{D(T,T_0)} \right) \right]. \tag{29}$$

Equations (19) and (29) have the stationary limits,

$$\langle w^2 \rangle \sim \begin{cases} c_0(T,T_0) \Delta t^{2\alpha(T)}, & \Delta t \ll t_w \\ c_\infty(T,T_0) \Delta t^{2\alpha(T)}, & \Delta t \gg t_w, \end{cases} \tag{30}$$

with

$$c_0(T,T_0) \equiv A(T,T_0) 10^{-B(T,T_0)},$$

$$c_\infty(T,T_0) \equiv A(T,T_0) 10^{B(T,T_0)}. \tag{31}$$

These parameters control the two stationary asymptotes bounding the aging regime. The parameter $2B(T,T_0) = \log_{10}[c_\infty(T,T_0)/c_0(T,T_0)]$ is then a measure of the distance between the two asymptotes.

Figure 6(b) shows the scaling plot of the averaged roughness in the growth regime. We display data for $L=5000$ at $T=0.5$ and $L=500$ at $T=0.2$. Note that the data for $L=500$ at $T=0.5$ shown in panel (a) of Fig. 6 would have not scaled properly since saturation appears earlier.

The temperature dependences of the (effective) growth exponent $\alpha$ as well as the parameter $B$ for the solid-on-solid model evolving from an infinite temperature initial condition are shown in Fig. 7. The exponent $\alpha$ approaches the EW value $2\alpha=1/2$ at high temperature. In the high-temperature limit the parameter $B(T,\infty)$ approaches zero since the two constants $c_0(T,\infty)$ and $c_\infty(T,\infty)$ tend to the same temperature-independent value and aging disappears.

Figure 8 shows the averaged two-time roughness for the continuous model with a high initial temperature $T_0=5$. The upper curve in Fig. 8(a) corresponds to the stationary case where the temperature is kept constant at the initial value. The other two cases, with $T=1$ and $T=0.5$, present aging which is qualitatively similar to the SOS model of Fig. 6. Figure 8(b) shows the scaling of these curves with the temperature-dependent exponents $\alpha$ given in the key. In the continuous model the exponent $\alpha$ increases with temperature until reaching the EW value $2\alpha=1/2$ at the crossover temperature $T_{co}(L)$. In Fig. 9(a) we present $\alpha(T)$ for the cases with a fixed initial temperature $T_0=5$. As can be observed, its precise temperature dependence is not easy to determine. Since one expects that the $\alpha$ exponent determines the slow

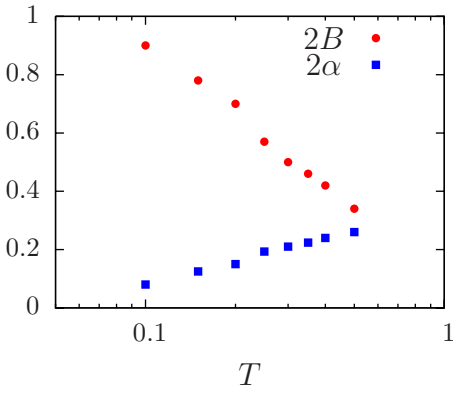


FIG. 7. (Color online) Temperature dependence of the effective growth exponent $\alpha$ and the parameter $B$ measuring the distance between the two asymptotes $c_0$ and $c_\infty$ in the lattice model evolving from an infinite temperature initial condition.

dynamics at a given temperature, it is interesting to check that the value of $\alpha$ at a small temperature does not depend on the initial temperature. This is shown in Fig. 9(b), where we show that $\alpha(T=0.5)$ is independent of the initial temperature. Although we do not compute the parameter $B$ for the continuous model, it is worth noting that in contrast with the discrete case the two constants $c_0$ and $c_\infty$ approach a

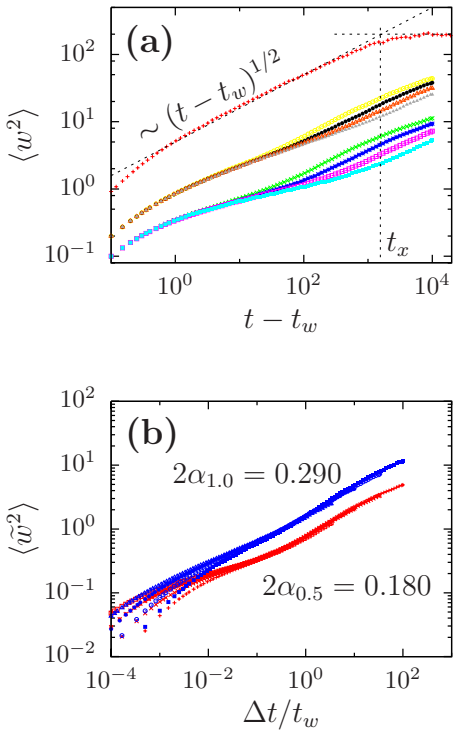


FIG. 8. (Color online) The averaged two-time roughness in the continuous model after a quench from high temperature $T_0=5$. (a) $L=256$ and different temperatures. The upper curve corresponds to the evolution of the roughness when the temperature is the same as the initial value, i.e., a stationary situation. Curves for $T=1$ (middle curves) and $T=0.5$ (lower curves) are shown. The waiting times are $t_w=100$, 300, 1000, and 3000 from left to right. (b) Scaling plot of the data presented for $T=1.0$ and $T=0.5$ using the $\alpha$ values given in the figure.

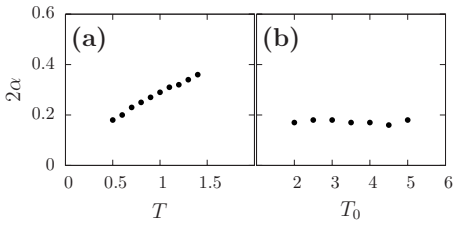


FIG. 9. Initial and working temperature dependence of the scaling exponent $\alpha$ in the continuous EW model in a random environment. (a) The initial temperature is fixed to $T_0=5$ and the working temperature is varied. (b) The exponent $\alpha$ does not change while changing the initial temperature $T_0$ and keeping the working temperature fixed at $T=0.5$.

temperature-dependent asymptote that equals the high-temperature limit of the EW line, $c_0 \propto 2T$ and $c_\infty \propto (2-\sqrt{2})T + \sqrt{2}T_0$.[18] The exponent $\alpha$ monotonically increases from $\alpha(T=0) \approx 0$ and crosses over to $2\alpha = 1/2$ at some $T_{co}(L)$ with a very weak $T$ dependence.

The effect of using as an initial configuration one in equilibrium at a lower temperature was considered analytically in Ref. 18 for the EW line. In presence of disorder one is often forced to use numerical simulations and the difficulty of equilibrating a long line at low temperature arises. However, a special case is that of the lattice model at $T_0=0$. It is indeed well known that its ground state configuration can be exactly calculated by transfer-matrix methods.[28]

In Fig. 10 we show the two-time roughness of the discrete disordered line using as initial configurations equilibrium ones at $T_0=0$ and a working temperature $T=0.2$. The plots demonstrate that the trend of the curves is to reverse in the sense that the curves go from the upper to the lower asymptote. This behavior is similar to what was found analytically for the clean EW line[18] and the KPZ nonlinear model.[20] This effect is also reminiscent of what was observed in the relaxation of the $2d$ $XY$ model from a uniform initial condition, corresponding to equilibrium at $T_0=0$, at finite (higher) temperature within the spin-wave approximation.[37]

The effect of the initial condition can be summarized in the following way. At all working temperatures that are identical to the one of the initial condition, $T=T_0$, one finds $c_0 = c_\infty$ and there is no aging since the line is initially in equilibrium.[18] For $T>T_0$ one has $c_0>c_\infty$, while for $T<T_0$ one has $c_0<c_\infty$. The values of these constants determine the relative location of the two asymptotes of the growth regime, $\Delta t \ll t_w$ and $\Delta t \gg t_w$.

### B. Linear response

We now turn to the study of the linear response. In Fig. 11 we show the averaged integrated linear response of the roughness in the lattice model. In panel (a) we show data for several waiting times as a function of time delay. In panel (b) we scale the data as

$$\langle \chi \rangle(t,t_w) \sim \ell^{2\zeta}(t_w) \langle \tilde{\chi} \rangle \left( \frac{\ell(t)}{\ell(t_w)} \right) \tag{32}$$

with $\ell(t) \sim t^{1/z}$.

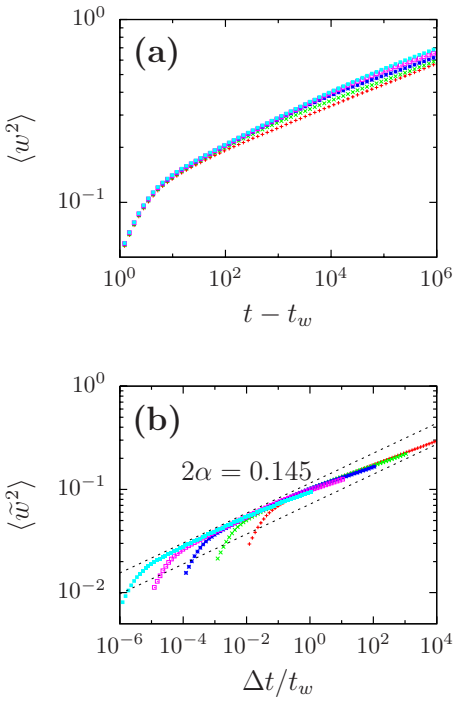


FIG. 10. (Color online) Panel (a): the averaged two-time roughness in the lattice model for an elastic line with length $L=5000$. Evolution at $T=0.2$ after a sudden heating from equilibrium at $T_0=0$. The waiting times are $t_w=10$ (plus, red), $t_w=10^2$ (cross, green), $t_w=10^3$ (star, blue), $t_w=10^4$ (open square, pink), and $t_w=10^5$ (filled square, cyan). Panel (b): scaling plot of the data in panel (a). Note that the value of $\alpha$ (in the key) coincides with the one used in the case of a quench to $T$ from $T_0 \to \infty$ (see Fig. 6). The dashed lines are the bounding asymptotes. Let us remark that, here, $c_\infty < c_0$.

These results are to be confronted with the behavior of the EW elastic line with Langevin dynamics for which the integrated linear response is *stationary* and does not fluctuate.[18] On the other hand, the linear response obtained with the continuous model, not shown here, is qualitatively similar to the one shown for the SOS model in Fig. 11.

In Fig. 12 we display data for the linear response after the sudden heating from the ground state used in Sec. IV A. The effect of this "reversed" heating procedure is similar to the one showed in Sec. IV A and in Fig. 10 for the roughness.

### C. FDT

The modification of the FDT linking the displacement to its associated response in the lattice model after a quench from infinite temperature was studied by Barrat[12] and Yoshino.[13,14] We here focus on the behavior of the roughness and its linear response. We show data for the disordered EW line after a similar quench. In Fig. 13 we show the plot $\langle \tilde{\chi} \rangle$ against $\langle \tilde{w}^2 \rangle$ at fixed $t_w$ and using $\Delta t$ as a parameter going from $\Delta t=0$ to $\Delta t \to \infty$ in the continuous disordered EW line for the cases $T_0=5$ and $T=0.5$. As it can be observed, it displays two slopes, allowing for the definition of an effective temperature.[7] A similar behavior was reported for the displacement and associated linear response in the lattice model,[13] the clean EW line,[18] and the vortex glass model.[6]

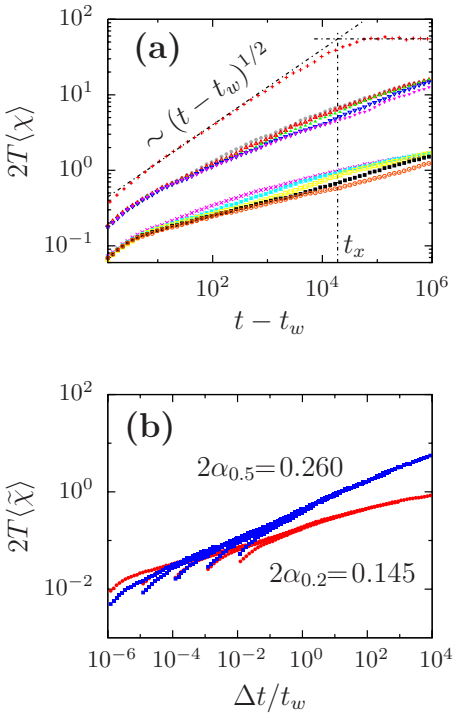


FIG. 11. (Color online) The noise and disordered averaged integrated linear response associated to the two-time roughness of the lattice elastic line. Panel (a): the line with length $L=500$ evolving at $T=5,0.5,0.2$ after a quench from infinite temperature, $T_0\to\infty$. Panel (b): scaling plot of the averaged two-time linear response of the line with $L=500$ and $T=0.2$ and the line with $L=5000$ and $T=0.5$.

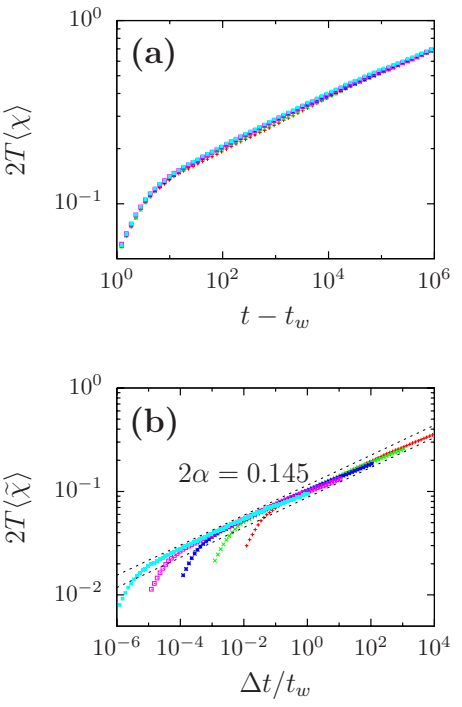


FIG. 12. (Color online) Panel (a): the averaged integrated linear response associated to the two-time roughness in the lattice model for an elastic line with $L=5000$. Evolution at $T=0.2$ after a sudden heating from equilibrium at $T_0=0$. The waiting times and symbols are as in Fig. 10. Panel (b): scaling plot of the data in (a). Note that the value of $\alpha$ (in the key) coincides with the one found in the study of $\langle w^2\rangle$ and the one used in the case of a quench to $T$ from $T_0\to\infty$ (see Figs. 6 and 10). The dashed lines are the bounding asymptotes. Let us remark that, here, $c_\infty<c_0$.

The temperature dependence of the effective temperature is shown in Fig. 14 for the disorder and the clean case. The dependence of $T_{\rm eff}$ on the working temperature while keeping $T_0$ fixed is shown in Fig. 14(a), but it is difficult to assess whether the effective temperature is constant or slowly grows with $T$. Without disorder the EW solution gives a linear dependence $T_{\rm eff}=T/\sqrt{2}+T_0(1+1/\sqrt{2})$,[18] shown with dashed lines in the figure. When the working temperature is fixed at $T=0.5$ and the initial temperature is changed, $T_{\rm eff}$ grows linearly with $T_0$, as shown in Fig. 14(b) and in the clean limit.

We also studied the effect of a heating procedure on the violations of the FDT using the lattice model. We show in Fig. 15 the parametric plot $\langle\tilde{\chi}\rangle$ against $\langle\tilde{w}^2\rangle$ using as initial condition the ground state at $T=0$. As already found in the clean EW line we find that $T_{\rm eff}<T$. $T_{\rm eff}$ thus reflects, consistently, a "memory" of the initial configuration.

## V. CROSSOVER-INDUCED GEOMETRICAL AND DYNAMICAL EFFECTS

We discuss here how our numerical results can be explained by developing simple scaling arguments based on the existence of a single dynamic crossover in the growing correlation length at a static temperature-dependent length $L_T$ from a thermally dominated regime to a disorder-dominated regime with algebraically growing barriers as a function of the length scale. The main additional assumption that we make is that at large enough length scales $\ell\gg L_T$, the geometry and typical barriers controlling the dynamics are indistinguishable from those at zero temperature. With these hypotheses, which are qualitatively supported by our numerical results, we can predict (i) the temperature dependence of $L_T$, (ii) the temperature dependence of the effective exponents characterizing each regime of growth, (iii) the temperature dependence of the crossover time between these regimes, and (iv) a parameter quantifying the importance of

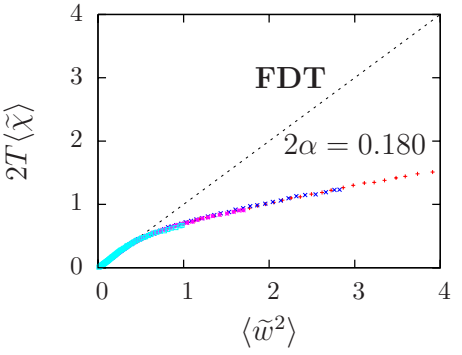


FIG. 13. (Color online) The parametric plot of the scaled linear response against the roughness for the continuous model with $T_0=5$ and $T=0.5$. The dashed line indicates the FDT limit.

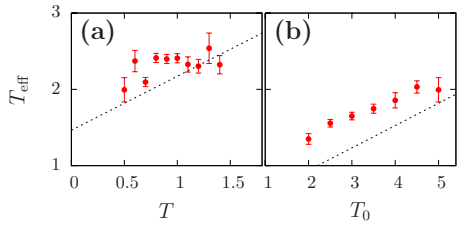


FIG. 14. (Color online) Temperature dependence of the effective temperature, signaling the violation of the FDT, comparing the clean EW system—dashed lines—with the disordered continuous case. (a) Dependence on the working temperature for a fixed initial temperature $T_0=5$. (b) Dependence on the initial temperature $T_0$ while the working temperature is kept fixed at $T=0.5$.

crossover-induced finite-size or finite-time effects in simulations. In order to make the discussion in this section self-contained we start by repeating some arguments that are well known in the literature and then we present the scenario that, we propose, explains the numerical observations.

If the temperature is high enough to renormalize the microscopic pinning parameters,[26] thermal fluctuations dominate the line wandering at short length scales. The geometry of equilibrated small scales, $\ell \ll L_T$, is thus described by the thermal roughness exponent $\zeta_T=1/2$ of the clean EW equation, such that $\langle w^2\rangle \sim (T/c)\ell$ for $\ell/L_T \ll 1$ or $S(q) \sim (T/c)q^{-(1+2\zeta_T)}$ for $qL_T \gg 1$ or $q \gg q_T \sim 1/L_T$. The typical time needed to equilibrate a length $\ell$ in this regime is therefore expected to be $t(\ell) \sim \ell^z$, with the EW dynamical exponent $z=2$.

At length scales $\ell \gg L_T$, disorder dominates and the geometry of the equilibrated large length scales, $\ell \gg L_T$, is the same as in the ground state, $S(q) \sim q^{-(1+2\zeta_D)}$ for $qL_T \ll 1$, with $\zeta_D=2/3 > \zeta_T$. The typical time to equilibrate a length $\ell \gg L_T$ is controlled by size-dependent *energy* barriers $U(\ell)$, such that $t(\ell) \sim e^{U(\ell)/T}$, with $U(\ell) \sim \ell^\psi \gg T$. By hypothesis, we assume that both the form of $S(q)$ and the barriers $U(\ell)$ are independent of $T$ in this regime, in agreement with what is seen in Fig. 1 for the structure factor with $q \ll q_T$.

In order to capture the crossover effects we interpolate the geometric and dynamic behaviors of the regimes $\ell \gg L_T$ and $\ell \ll L_T$ described above. The static structure factor can be written as

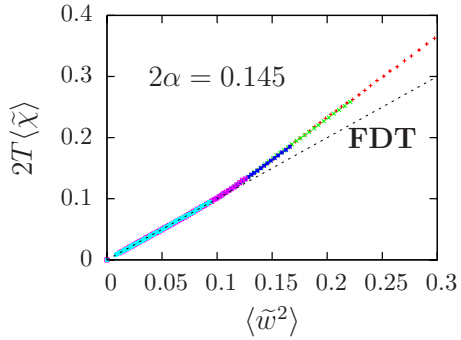


FIG. 15. (Color online) The parametric plot $2T\langle\tilde{\chi}\rangle$ against $\langle\tilde{w}^2\rangle$ after a heating procedure from the ground state at $T_0=0$ to $T=0.2$ in the SOS model. The waiting times are 10 MCs (plus, red), $10^2$ MCs (cross, green), $10^3$ MCs (star, blue), $10^4$ MCs (open square, pink) and $10^5$ MCs (filled square, cyan). Note that $T_{\rm eff} < T$.

$$S(q,T) \sim q^{-(1+2\zeta_D)} g(qL_T,T) \tag{33}$$

with $g(x,T) \sim Tx^{2(\zeta_D-\zeta_T)}$ for $x \gg 1$ and $g(x,T) \sim$ const for $x \ll 1$. This interpolating form, which includes the temperature, is found to fit well the data and to satisfy our assumption $S(q,T) \approx S(q,T=0)$ for $qL_T \ll 1$. We continuously match the two regimes by requiring $q_T^{-(1+2\zeta_D)} = Tq_T^{-(1+2\zeta_T)}$ and, therefore,

$$L_T \sim T^{1/\phi} = T^3, \tag{34}$$

with $\phi=2(\zeta_D-\zeta_T)=1/3$, which is the temperature dependence of the crossover length we observe in Fig. 2. This argument was also discussed in Sec. III B 2 on numerical grounds, where references were also given.

Let us now discuss the dynamical behavior induced by $L_T$. At the crossover we can roughly set $U(L_T) \sim T$ since barriers start to dominate the dynamics only above $L_T$. For $\ell \gg L_T$ we expect $U(\ell) \sim \ell^\psi \gg T$. To interpolate the large scale behavior down to $L_T$ we use[26]

$$U(\ell) \sim T(\ell/L_T)^\psi. \tag{35}$$

Since by hypothesis $U(\ell,T) \approx U(\ell,T=0)$ for $\ell \gg L_T$, we obtain $\psi=\phi=2(\zeta_D-\zeta_T)$. It is worth noting here that this result relates dynamics and statics since $\theta=2\zeta_D-1 \equiv 2(\zeta_D-\zeta_T)$ is also the static exponent describing the sample-to-sample equilibrium free-energy fluctuations. This analysis thus suggests that $\psi \approx \phi \approx \theta = 1/3$.

Using the previous arguments, the time to equilibrate a length $\ell$ can hence be written as

$$t(\ell) \sim e^{(\ell/L_T)^\psi} \ell^z. \tag{36}$$

This expression continuously matches the barrier-dominated regime, $t \sim \exp[(\ell/L_T)^\psi] = \exp[\ell^\psi/T]$ for $\ell \gg L_T$, with the power-law growth expected in the thermal regime, $t \sim \ell^z$ for $\ell \ll L_T$. From Eq. (36) and using $L_T \sim T^{1/\phi}$ one obtains a characteristic time scale,

$$t_\times \sim L_T^z \sim T^{z/\psi} = T^6, \tag{37}$$

separating thermally from disorder-dominated dynamics. This strong temperature dependence explains why the crossover to the slow logarithmic growth is particularly difficult to observe in numerical simulations. On the one hand, at high temperature, the line size must be large $L > L_T \sim T^3$ in order to see the crossover to the long-time logarithmic regime. On the other hand, at low temperature, the lines could in principle cross over to the logarithmic regime even for small system sizes but, because of the very slow Arrhenius activated dynamics, exceedingly long running times would be needed to resolve the precise time dependence. Most importantly, the data from any numerical simulation displaying the two regimes of growth will be characterized by temperature-dependent effective exponents due to crossover-induced finite-size and finite-time effects, as we explain below.

Indeed, Eq. (36) allows us to explain the temperature dependence in the effective exponents of the power-law and logarithmic growth regimes. The influence of the crossover in the effective dynamic exponent $\tilde{z}$ of the power-law regime relevant to short length scales, $\ell \ll L_T$, follows from equating Eq. (36) to $t(\ell) \sim \ell^{\tilde{z}}$, which yields

$$\tilde{z} - z \approx \frac{(\ell^{\psi}/\ln \ell)}{L_T^{\psi}} \approx \frac{(\tilde{z} t^{\psi/\tilde{z}}/\ln t)}{L_T^{\psi}}. \tag{38}$$

To avoid solving the resulting self-consistent equation, we can use $\tilde{z} \approx z$ in the third member to obtain a first-order correction to the dynamic exponent,

$$\tilde{z} - z \approx \frac{(z t^{\psi/z}/\ln t)}{L_T^{\psi}}. \tag{39}$$

Since by construction the power-law fit of the data is done in a relatively short time-scale such that $t^{\psi/z}/\ln t$ is almost constant (otherwise $\tilde{z}$ would not be well defined) and by using $L_T \sim T^3$ and $\psi = 1/3$, we get

$$\tilde{z} - 2 \simeq T^{-1}. \tag{40}$$

This rough estimate is in good agreement with the numerically determined exponent $\alpha$ shown in Figs. 7 and 9.

It is worth noting here that the Cardy-Ostlund random Sine-Gordon model[29] in $d=2$, disordered ferromagnets,[30] and Ising and vector spin glasses[31] were shown to display a dynamic exponent $z \sim 2 + a/T$, with $a$ of the order of unity and depending on details of the considered model. Our arguments and numerical study show that the numerically measured dynamic exponent in our system could simply be an effective value that stems from the interpolation of two growth regimes that cannot be properly resolved numerically. We cannot, however, directly apply the same arguments to explain the similar behavior of the dynamic exponent in the above systems. On one hand, the Cardy-Ostlund model in $d=2$ has, in the pinned phase, $\theta=0$ (i.e., the glass phase is marginal), so if $\psi \sim \theta = 0$ is true in this system, the growth of barriers is strictly logarithmic[29] rather than the algebraic growth we are assuming in our arguments. On the other hand, disordered ferromagnets such as analyzed in Ref. 30 or vector spin glasses[31] are strongly disordered systems, and it is therefore not obvious how to relate their behavior with the one of a (weakly pinned) directed elastic manifolds with one transverse direction such as the 1+1 elastic string we study or the 2+1 elastic interface of the $d=2$ Cardy-Ostlund model, which can be described by the $d$-dimensional generalization of Eq. (1). Moreover, we are not aware of the observation in these systems of a geometrical crossover from a thermally dominated to a disorder-dominated length-scale regime, which is a necessary input in our arguments. It seems that our arguments are particularly important for systems with a positive barrier exponent $\psi$ displaying a crossover from a thermally dominated short-time regime where the correlation length grows as a power law, to a long-time dynamics dominated by algebraically diverging energetic barriers, with a logarithmically growing correlation length. This could be realized in disordered ferromagnets or other system displaying well-defined domain walls in the weak disorder limit. Why the crossover-induced effective exponents we found appear to be quite similar to the one found in a true marginal glass phase or in some spin glass model is an interesting open question though.

The seemingly paradoxical temperature dependence of the effective exponent in the regime of logarithmic growth, $\ell \gg L_T$, shown in Fig. 4, can be explained with a similar argument. By equating Eq. (36) to $t(\ell) \sim \exp[\ell^{\tilde{\psi}}/T]$ we find

$$\tilde{\psi} - \psi \approx \frac{\ln[T/L_T^{\psi} + zT \ln \ell/\ell^{\psi}]}{\ln \ell}. \tag{41}$$

We use now $L_T \sim T^3$ and the time dependence $\ell \sim (T \ln t)^{1/\tilde{\psi}}$ in the second member to get a self-consistent equation for $\tilde{\psi}$, namely,

$$\tilde{\psi} - \psi \sim \frac{\tilde{\psi}}{\ln(T \ln t)} \ln\left[1 + \frac{Tz}{\tilde{\psi}} \frac{\ln(T \ln t)}{(T \ln t)^{\psi/\tilde{\psi}}}\right]. \tag{42}$$

Setting $\tilde{\psi} \approx \psi$ in the second member we obtain a first-order approximation for $\tilde{\psi} - \psi$,

$$\tilde{\psi} - \psi \sim \frac{\psi}{\ln(T \ln t)} \ln\left[1 + \frac{z}{\psi} \frac{\ln(T \ln t)}{\ln t}\right]. \tag{43}$$

At high temperatures (or large times) such that $T \ln t \gg 1$ this expression simply yields $\tilde{\psi} \sim \psi$. In the opposite low $T$ limit for sufficiently large length/time scales such that the restriction $\ell(t) \gg L_T \sim T^3$ is still satisfied one finds $\tilde{\psi} > \psi$. Indeed, $\tilde{\psi}$ is a decreasing function of $T$. These argument is consistent with the result shown in Fig. 4, where we observe that $\tilde{\psi} > \psi$ at low temperatures and $\tilde{\psi} \to \psi = 1/3$ increasing the temperature.

The effective exponent analysis made above reveals that crossover-induced effects are controlled by the order of magnitude of $\ell^{\psi}/\ln \ell$. Since $\ell$ in a simulation is always a fraction of the system size $L$, a temperature dependence of the effective exponents can be expected for systems such that $L^{1/3}/\ln L \sim O(1)$. For instance, in order to properly resolve the dynamic exponent $z=2$ at short length scales we need $\ell \ll L_T$ for at least a few orders of magnitude range of $\ell$, i.e., a large $L_T$. On the other hand, to properly resolve the exponent $\psi$ we need $\ell^{1/3}/\ln \ell \gg 1$ for $L > \ell > L_T$ for at least a few orders of magnitude of $\ell$. Typically, the largest systems analyzed numerically in the literature have $L \sim O(10^3)$, with $L^{1/3}/\ln L \sim O(1)$, and do not satisfy the latter constraint. This clearly prompts for a careful interpretation of the anomalous temperature dependence of power-law or logarithmic growth exponents obtained numerically so far, as we discuss below.

In Ref. 13 the aging dynamics of an elastic string was numerically studied, by Monte Carlo simulation of a solid-on-solid model, for a line of size $L=500$. In this work the dynamics of the Fourier mode with zero wave vector was found to display a clear crossover from linear to nonlinear response, compatible with a power-law growth of barriers at large times and a crossover from power-law to logarithmic growth of the correlation length. However, the data for the relaxation of nonzero Fourier modes were analyzed in terms of an algebraically growing correlation length, arguing that a logarithmic law should be inaccurate since it is based in the hypothetic existence of a typical energy barrier. From the above analysis, this intriguing result can be explained by

taking into account that $L=500$ is still too small to avoid crossover-induced effects. Indeed, the temperature dependence of the dynamic exponent described here is compatible with our prediction for an effective dynamic exponent. We are thus not forced to abandon the simple interpretation in terms of a typical barrier growing algebraically with the length scale if we take into account the importance of crossover-induced effects in small systems.

In Ref. 34 the relaxation of an elastic line in a disordered potential was analyzed for the particular case $t_w=0$ and $T=0.5$. The crossover to the logarithmic growth was observed, though with an effective exponent $\tilde{\psi}\approx 0.49>\theta$. In Ref. 36 scaling arguments for the free energy of droplet excitations were given favoring the value $\psi=1/2$, against the commonly accepted value $\psi=\theta=1/3$,[28] in apparent agreement with the results in Ref. 34. In the present work we find not only $\tilde{\psi}\sim 0.51$ for $t_w=0$ and $T=0.5$, consistent with the result in Ref. 34, but also a decrease toward a value close to $\psi=1/3$ with temperature. This behavior is opposite to what is proposed in Ref. 36, where entropic effects leading to the value $\psi=1/2$ are expected to grow with $T$ from the $T=0$ value $\psi=\theta=1/3$ to the entropically driven value $\psi=1/2$. The scaling arguments given above thus show that the anomalous temperature dependence of $\tilde{\psi}$ can still be interpreted without dropping the $\psi=\theta=1/3$ identification, which was proposed some time ago.[28]

In numerical simulations of the steady-state slow driven motion of an elastic line[38] the effective creep exponent $\mu$ was found to be temperature dependent. According to the assumption $U(\ell)\sim \ell^{\theta}$ at large length scales, simple scaling arguments lead to $\mu=\theta/(2-\zeta_D)=1/4$ (see, for instance, Ref. 39). Taking into account that $L^{1/3}/\ln L\sim O(1)$ in those simulations we can expect, following an equivalent line of reasoning as above, a temperature-dependent effective creep exponent $\tilde{\mu}=\tilde{\psi}/(2-\zeta_D)>\mu$, such that $\tilde{\mu}\to\mu$ when $T$ grows. This behavior is in good qualitative agreement with the results in Ref. 38. Therefore, the anomalous temperature dependence observed in Ref. 38 cannot be used as evidence against obtaining the creep exponent entirely as a function of static exponents, although the large-scale geometry in the creep regime is found to be described by depinning exponents.[38,40]

## VI. CONCLUSIONS

Elastic manifolds are objects that appear in a large variety of problems with glassy features. It was shown in the past that these systems present aspects of glassy dynamics combined with diffusion properties.[6,11–15,18–20]

After a series of analytic and numerical studies of continuous and discrete models with and without quenched disorder we can summarize the main features of the out of equilibrium relaxation of individual and interacting directed one-dimensional objects.

All these systems age below a characteristic temperature $T_{co}(L)$. In the mean-field limit of an infinite number of transverse dimensions, for a line with infinite length, a dynamic phase transition arises at $T_{co}(L)$. Below $T_{co}(L)$ the lines age without diffusion.[11]

The dynamics of finite length lines moving in finite dimensional spaces cross over from diffusive-aging growth to a regime in which the roughness saturates. This phenomenon can be described with a generalization of the Family-Vicsek scaling.[6,18] The qualitative features of the two-time freely relaxing observables are generic and do not depend on the presence of quenched randomness but the details such as the exponents and growing length do. We performed a careful analysis of the time-dependent growing length and we found a crossover from an effective power law with temperature-dependent exponent to the expected asymptotic logarithmic growth for sufficiently long strings. Our numerical data indicate a temperature-dependent effective barrier exponent $\tilde{\psi}$, which is higher than the energy exponent $\theta=1/3$ at low temperatures but tends to it at high temperatures, provided the system is large enough to display the asymptotic behavior. As we discussed via scaling arguments this behavior can be recast in terms of crossover-induced effects, and it is not inconsistent with the usual assumption $\psi=\theta$ for this system.

We also found a single crossover length $L_T\sim T^3$ separating a thermally dominated regime with $\zeta_T=1/2$ and a disorder-dominated regime with the $T=0$ roughness exponent $\zeta_D=2/3$. We showed that this is consistent with the assumption that large scale properties of the system are indistinguishable from those at $T=0$. Translating this crossover into the dynamics we could also describe the temperature dependence of the effective dynamic exponents in the power-law growth regime and in the logarithmic growth regime. In this respect it would be important to study the corresponding crossover in $(1+2)$ dimensions, relevant for vortices in superconductors. This is crucial for high-$T_c$ superconductors where thermal fluctuations are known to strongly renormalize the disorder and produce Larkin lengths growing exponentially fast with temperature.[5] As the Larkin length marks the onset of metastability and the crossover to a barrier-dominated (random-manifold) regime, as it does $L_T$ in our case, we can expect the phenomenology and crossover-induced effects we describe here to be experimentally relevant, especially at the onset of irreversibility, near the transition to the vortex liquid phase,[5,6] where the Larkin length can become comparable with the sample size.[41]

The importance of measuring linear responses was demonstrated by the fact that all known coarsening systems (above their lower critical dimension) have an asymptotically vanishing linear response in the aging regime, in contrast to solvable mean-field glassy models and numerical simulations of finite dimensional glasses that yield a finite integrated linear response in the same two-time regime (see, e.g., Refs. 8 and 42). This fact appears as a concrete difference between the relaxation dynamics of coarsening and glassy systems.

The relaxation of the integrated thermal averaged linear response of elastic manifolds strongly depends on the presence or absence of quenched disorder. Mean-field elastic manifold models in quenched random environments have a fully aging linear response. The clean EW line has a stationary linear response, while the dirty continuous or lattice models have integrated linear responses with aging and diffusion combined.

The effective temperature[7] defined from the comparison of induced and spontaneous averaged fluctuations is finite in

all the cases considered as long as the diffusive factors in the correlations and linear responses are divided away. We also showed that the effective temperature is higher than the bath temperature for cooling procedures and, inversely, it is lower than the bath temperature for heating procedures. This is similar to what has been previously found in the $2d$ *XY* model[37] and the Edwards-Wilkinson elastic line[18] and gives support to the notion of effective temperature as measured from deviations from the fluctuation-dissipation relation.

The study of dynamic fluctuations in these systems has not been fully developed yet. In Ref. 15 we analyzed the fluctuations of the two-time roughness of the lattice disordered model during growth. The equilibrium[43] and out of equilibrium[18] roughness fluctuations in the EW line show a similar pattern. The probability distribution functions in all these models satisfy a scaling law and the scaling function follows the same trend as a function of all its variables. The question then arises as to whether the fluctuations of the linear responses of clean and disordered elastic lines are similar or different. We shall discuss this problem in a separate publication. The relation with the theory of fluctuations based on time-reparametrization invariance[44] will also be discussed elsewhere.

## ACKNOWLEDGMENTS

We thank D. Domínguez, T. Giamarchi, H. Rieger, A. Rosso, G. Schehr, and H. Yoshino for very useful discussions. L.F.C. thanks the Universidad Nacional de Mar del Plata, Argentina; S.B. and J.L.I. thank the Laboratoire de Physique Théorique et Hautes Energies, Université Pierre et Marie Curie Paris VI for hospitality during the preparation of this work. S.B. also thanks the University of Genève and the DPMC, where part of this work was initiated and the Swiss NSF under MaNEP and Division II for support. The authors acknowledge financial support from ANPCyT Grant No. PICT20075 and CONICET Grant No. PIP5648 (J.L.I.) and SECyT-ECOS Grant No. P.A01E01/A08E03 and PICS Grant No. 3172 (L.F.C.). L.F.C. is a member of Institut Universitaire de France.

[1] A.-L. Barabási and H. E. Stanley, *Fractal Concepts in Surface Growth* (Cambridge University Press, Cambridge, 1995); T. Halpin-Healey and Y.-C. Zhang, Phys. Rep. **254**, 215 (1995).
[2] A. J. Bray, Adv. Phys. **43**, 357 (1994).
[3] A. Hansen, E. L. Hinrichsen, and S. Roux, Phys. Rev. Lett. **66**, 2476 (1991); E. Bouchaud, J. Phys. Condens. Matter **9**, 4319 (1997); M. Alava, P. K. V. V. Nukalaz, and S. Zapperi, Adv. Phys. **55**, 349 (2006).
[4] L. C. E. Struick, *Physical Aging in Amorphous Polymers and Other Materials* (Elsevier, Amsterdam, 1978).
[5] G. Blatter, M. V. Feigel'man, V. B. Geshkenbein, A. I. Larkin, and V. M. Vinokur, Rev. Mod. Phys. **66**, 1125 (1994); T. Nattermann and S. Scheidl, Adv. Phys. **49**, 607 (2000); T. Giamarchi and P. Le Doussal, in *Spin Glasses and Random Fields*, edited by A. P. Young (World Scientific, Singapore, 1997).
[6] S. Bustingorry, L. F. Cugliandolo, and D. Domínguez, Phys. Rev. Lett. **96**, 027001 (2006); Phys. Rev. B **75**, 024506 (2007).
[7] L. F. Cugliandolo, J. Kurchan, and L. Peliti, Phys. Rev. E **55**, 3898 (1997).
[8] L. F. Cugliandolo, in *Slow Relaxations and Nonequilibrium Dynamics in Condensed Matter*, Ecole de Physique Les Houches Vol. 77, edited by J.-L. Barrat *et al.* (Springer, Berlin, 2003); also available as arXiv:cond-mat/0210312.
[9] F. Portier, G. Kriza, B. Sas, L. F. Kiss, I. Pethes, K. Vad, B. Keszei, and F. I. B. Williams, Phys. Rev. B **66**, 140511(R) (2002); R. Exartier and L. F. Cugliandolo, *ibid.* **66**, 012517 (2002).
[10] X. Du, G. Li, E. Y. Andrei, M. Greenblatt, and P. Shuk, Nat. Phys. **3**, 111 (2007).
[11] L. F. Cugliandolo and P. Le Doussal, Phys. Rev. E **53**, 1525 (1996); L. F. Cugliandolo, J. Kurchan, and P. Le Doussal, Phys. Rev. Lett. **76**, 2390 (1996); Z. Konkoli, J. Hertz, and S. Franz, Phys. Rev. E **64**, 051910 (2001); Z. Konkoli and J. Hertz, *ibid.* **67**, 051915 (2003); Y. Y. Goldschmidt, *ibid.* **74**, 021804 (2006).
[12] A. Barrat, Phys. Rev. E **55**, 5651 (1997).
[13] H. Yoshino, J. Phys. A **29**, 1421 (1996); Phys. Rev. Lett. **81**, 1493 (1998).
[14] H. Yoshino (unpublished).
[15] S. Bustingorry, J. L. Iguain, C. Chamon, L. F. Cugliandolo, and D. Domínguez, Europhys. Lett. **76**, 856 (2006).
[16] F. Family and T. Vicsek, J. Phys. A **18**, L75 (1985).
[17] S. F. Edwards and D. R. Wilkinson, Proc. R. Soc. London, Ser. A **381**, 17 (1982).
[18] S. Bustingorry, L. F. Cugliandolo, and J. L. Iguain, J. Stat. Mech.: Theory Exp. 2007, P09008.
[19] A. Röthlein, F. Baumann, and M. Pleimling, Phys. Rev. E **74**, 061604 (2006); **76**, 019901(E) (2007).
[20] S. Bustingorry, J. Stat. Mech.: Theory Exp. 2007, P10002.
[21] See also J. J. Ramasco, J. M. López, and M. A. Rodríguez, Europhys. Lett. **76**, 554 (2006).
[22] M. Kardar, G. Parisi, and Y.-C. Zhang, Phys. Rev. Lett. **56**, 889 (1986).
[23] A. Rahmani, C. Castelnovo, J. Schmit, and C. Chamon, J. Stat. Mech.: Theory Exp. 2007, P09022.
[24] D. Loi, S. Mossa, and L. F. Cugliandolo, Phys. Rev. E **77**, 051111 (2008).
[25] A. Rosso and W. Krauth, Phys. Rev. E **65**, 025101(R) (2002).
[26] T. Nattermann, Y. Shapir, and I. Vilfan, Phys. Rev. B **42**, 8577 (1990).
[27] A. B. Kolton, R. Exartier, L. F. Cugliandolo, D. Domínguez, and N. Gronbech-Jensen, Phys. Rev. Lett. **89**, 227001 (2002).
[28] M. Kardar, Phys. Rev. Lett. **55**, 2923 (1985); B. Drossel and M. Kardar, Phys. Rev. E **52**, 4841 (1995).
[29] G. Schehr and P. Le Doussal, Phys. Rev. E **68**, 046101 (2003); Phys. Rev. Lett. **93**, 217201 (2004); Europhys. Lett. **71**, 290 (2005); G. Schehr and H. Rieger, Phys. Rev. B **71**, 184202 (2005).
[30] M. Henkel and M. Pleimling, Europhys. Lett. **76**, 561 (2006); Phys. Rev. B **78**, 224419 (2008).
[31] H. G. Katzgraber and I. A. Campbell, Phys. Rev. B **72**, 014462

(2005).
[32] M. Müller, D. A. Gorokhov, and G. Blatter, Phys. Rev. B **63**, 184305 (2001); **64**, 134523 (2001).
[33] E. Agoritsas, Master thesis, University of Geneva, 2008.
[34] A. B. Kolton, A. Rosso, and T. Giamarchi, Phys. Rev. Lett. **95**, 180604 (2005).
[35] T. Nogawa, K. Nemoto, and H. Yoshino, Phys. Rev. B **77**, 064204 (2008).
[36] C. Monthus and T. Garel, J. Phys. A **41**, 115002 (2008).
[37] L. Berthier, P. W. C. Holdsworth, and M. Sellitto, J. Phys. A **34**, 1805 (2001).
[38] A. B. Kolton, A. Rosso, and T. Giamarchi, Phys. Rev. Lett. **94**, 047002 (2005).
[39] T. Giamarchi, A. B. Kolton, and A. Rosso, Lect. Notes Phys. **688**, 91 (2006).
[40] A. B. Kolton, A. Rosso, T. Giamarchi, and W. Krauth, Phys. Rev. Lett. **97**, 057001 (2006).
[41] M. I. Dolz and H. Pastoriza (private communication).
[42] F. Corberi, E. Lippiello, and M. Zannetti, J. Stat. Mech.: Theory Exp. 2004, P12007.
[43] Z. Rácz, Proc. SPIE **5112**, 248 (2003).
[44] C. Chamon and L. F. Cugliandolo, J. Stat. Mech.: Theory Exp. 2007, P07022.